tapraid5/z8q-polyphy/z8q-polyphy/z8q00604/z8q2785d04g | gockleyj | S=15 | 12/17/03 | 13:51 | Art: 03090532 | Input-DCT-???

Thermodynamic Analysis of the Phase Separation during the Polymerization of a Thermoset System into a Thermoplastic Matrix. II. Prediction of the Phase Composition and the Volume Fraction of the Dispersed Phase

CARMEN CRISTINA RICCARDI,[1] JULIO BORRAJO,[1] LAURE MEYNIE,[2] FRANÇOISE FENOUILLOT,[2] JEAN-PIERRE PASCAULT[2]

[1]Institute of Materials Science and Technology, University of Mar del Plata and National Research Council, J. B. Justo 4302, B7608FDQ Mar del Plata, Argentina

[2]Laboratoire des Matériaux Macromoléculaires, UMR-CNRS 5627, Institut National des Sciences Appliquées, 17 Avenue Jean Capelle, 69 621 Villeurbanne Cedex, France

Received 24 September 2003; revised 3 November 2003; accepted 10 November 2003
Published online 00 Month 2004 in Wiley InterScience (www.interscience.wiley.com). DOI: 10.1002/polb.20003

ABSTRACT: A thermodynamic simulation of the phase-separation process of an off-critical blend, based on a thermoplastic matrix with a reactive epoxy system undergoing polycondensation at a constant temperature, was performed. The model considered the composition dependence of the interaction parameter, $\chi(T,\Phi_2)$ (where T is the temperature and Φ_2 is the volume fraction of polystyrene), along with the polydispersity of both polymers. For every level of conversion, the simulation provided the amount, composition, stoichiometric ratio, and conversion of each phase present. The accuracy of the model was proved by the good agreement between the experimental and predicted glass-transition temperatures and heat capacity changes at the glass-transition temperatures for both phases © 2003 Wiley Periodicals, Inc. J Polym Sci Part B: Polym Phys 42: 000–000, 2004

Keywords: phase separation; simulations; epoxy-modified polystyrene; polydisperse polymers; thermal properties

Author Proof

INTRODUCTION

Venderbosch et al.[1] demonstrated that epoxy systems can be applied as reactive solvents for thermoplastics by improving their processability; that is, the solvent reduces the viscosity and the high processing temperatures that are normally required. In addition, the polymerization of an epoxy monomer initiates a phase-separation process, which develops morphologies that determine the properties of the final material.

As a result of phase separation, various types of phase-separated structures can be formed, depending on several factors, including the composition, the rate of polymerization, the types of materials used, and physical properties, such as the viscosity and rate of diffusion.[2] One important factor controlling the phase-separation process and the morphologies generated is the location of the composition of the initial blend. For compositions near the critical composition, the reaction proceeds to drive the system into the unstable region of the phase diagram, the phase separation occurs by spinodal decomposition, and the structures formed display connectivity. For off-critical compositions, as is usual in formulations when a

Correspondence to: C. C. Riccardi (E-mail: criccard@fi.mdp.edu.ar)

© 2003 Wiley Periodicals, Inc.

reacting thermosetting polymer is used as a reactive solvent for a thermoplastic polymer, the second phase appears through nucleation and growth (NG).[3] Reaction-induced phase separation is a complex phenomenon: it is induced by the thermodynamic instability, but the resulting morphology is codetermined by the ratio of the rate of phase separation to the rate of the chemical reaction.[4] The NG mechanism can become completely inhibited when the rate of diffusion is very low, but if the temperature of reaction is well selected, the phase-separation process occurs faster than the reaction.

Meynie et al.[5] followed the morphology development of a blend based on a thermoplastic matrix with a reactive system undergoing polymerization. The system consisted of 60 wt % polystyrene (PS) mixed with 40 wt % reactive mixtures of epoxy monomers based on diglycidyl ether of bisphenol A (DGEBA) with stoichiometric amounts of 4,4′-methylenebis(2,6-diethylaniline) (MDEA). Experiments were carried out in a temperature-controlled oil bath and in an internal mixer. In the first case, the reaction-induced phase-separation process was conducted under quiescent conditions, and in the second case, it was performed under dynamic conditions. Upon phase separation, dispersed droplets of epoxy–amine were formed, which grew in size and number. Two phases coexisted: a PS-rich phase (the α phase) and an epoxy-rich phase (the β phase). Although the final morphologies were quite different, depending on the shear, the mean value of the epoxy conversion (p), the surface fraction of the dispersed-phase particles, and the glass-transition temperature (T_g) of the two phases were the same for the quiescent and dynamic systems. Thus, the evolution of the reaction and the phase compositions for the static and dynamic blends were the same, and this meant that they were not controlled by diffusion processes. In the first part of this work,[6] we applied a thermodynamic model to the phase-separation process for this system, considering the composition dependence of the interaction parameter and the polydispersity of both polymers.

In a previous work,[7] a thermodynamic simulation of the phase-separation process in a modified thermosetting polymer was carried out. For every level of conversion, the simulation provided the amount, composition, stoichiometric ratio (r), and conversion of the phases present. The aim of this work is to apply such a thermodynamic simulation to the particular system studied by Meynie et al.;[5] we model the evolution of the volume fractions and the composition of the dispersed phase and use the results to predict the evolution of the thermal properties.

EXPERIMENTAL

The material characterization, blend composition, preparation, and experimental techniques have been described elsewhere.[5,7]

The experimental volume fractions of the dispersed domains were obtained from an analysis of transmission electron microscopy (TEM) pictures. With TEM pictures, we directly determined the volume fraction of the dispersed phase [i.e., the volume fraction of the β phase (V_β)], using the surface ratio and assuming that this ratio was valid for three-dimensional space.[8] About 150 particles were analyzed.

THERMODYNAMIC MODEL

In the first part of this work,[6] we applied a thermodynamic model to the phase-separation process of reactive mixtures (polymer 1) of epoxy monomers based on DGEBA with stoichiometric amounts of MDEA mixed with PS (polymer 2). For a fluid mixture of two polydispersed polymers, with volume fractions given by

$$\Phi_1 = \sum_{i=1}^{m} \phi_i \quad \text{and} \quad \Phi_2 = \sum_{j=1}^{n} \phi_j \tag{1}$$

the model was applied, with consideration given to the composition dependence of the interaction parameter, $\chi(T,\Phi_2)$ (where T is the temperature and Φ_2 is the volume fraction of PS), and the polydispersity of both polymers. In this analysis, $\chi(T,\Phi_2)$ was considered the product of two functions, one depending on the temperature [$D(T)$] and the other depending on the composition [$B(\Phi_2)$]:[9–12]

$$\chi = D(T)B(\Phi_2)$$

$$\chi = \left(d_0 + \frac{d_1}{T}\right) \frac{1}{1 - b\Phi_2} \tag{2}$$

Coexistence curves were obtained from the expression of the Gibbs free energy change of mix-

Author Proof

tapraid5/z8q-polyphy/z8q-polyphy/z8q00604/z8q2785d04g | gockleyj | S=15 | 12/17/03 | 13:51 | Art: 03090532 | Input-DCT-???

ing arising from the model of Koningsveld and Kleintjens,[13] as described in the first part of this work.[6] The equations for the separation factors, σ_1 and σ_2, are as follows:

$$\sigma_1 = \frac{1}{Z_i}\ln\frac{\phi_i^\beta}{\phi_i^\alpha} = \left(\sum_{i=1}^{m}\frac{\phi_i^\beta}{Z_i} + \sum_{j=1}^{n}\frac{\phi_j^\beta}{Z_j}\right) - \left(\sum_{i=1}^{m}\frac{\phi_i^\alpha}{Z_i} + \sum_{j=1}^{n}\frac{\phi_j^\alpha}{Z_j}\right) + D(T)\left(\frac{\Phi_2^{\alpha 2}}{1-b\Phi_2^\alpha} - \frac{\Phi_2^{\beta 2}}{1-b\Phi_2^\beta}\right) \quad (3)$$

$$\sigma_2 = \frac{1}{Z_j}\ln\frac{\phi_j^\beta}{\phi_j^\alpha} = \left(\sum_{i=1}^{m}\frac{\phi_i^\beta}{Z_i} + \sum_{j=1}^{n}\frac{\phi_j^\beta}{Z_j}\right) - \left(\sum_{i=1}^{m}\frac{\phi_i^\alpha}{Z_i} + \sum_{j=1}^{n}\frac{\phi_j^\alpha}{Z_j}\right) + D(T)\left(\frac{1}{b}\ln\frac{1-b\Phi_2^\alpha}{1-b\Phi_2^\beta} + \frac{\Phi_1^\beta\Phi_2^\beta}{1-b\Phi_2^\beta} - \frac{\Phi_1^\alpha\Phi_2^\alpha}{1-b\Phi_2^\alpha}\right) \quad (4)$$

where ϕ_i and ϕ_j are the volume fractions of the i-mer and j-mer, respectively, and Z_i and Z_j are the number of lattice sites occupied by them:

$$\phi_i^\beta = \phi_i^\alpha\exp(\sigma_1 Z_i) \quad \text{and} \quad \phi_j^\beta = \phi_j^\alpha\exp(\sigma_2 Z_j) \quad (5)$$

During the phase-separation process, the distribution of i species of polymer 1 between the α and β phases must satisfy the following balance:

$$\phi_i^0 = (1 - V_\beta)\phi_i^\alpha + V_\beta\phi_i^\beta \quad (6)$$

where ϕ_i^0 is the initial volume fraction of species i.

Substituting σ_1, defined by eq 3, into eq 6 and rearranging, we obtain

$$\phi_1^\alpha = \sum_{i=1}^{m}\phi_i^\alpha = \sum_{i=1}^{m}\frac{\phi_i^0}{1 + V_\beta[\exp(\sigma_1 Z_i) - 1]} \quad (7)$$

In a similar way, ϕ_i^β and ϕ_1^β can be obtained from eqs 3 and 6 as follows:

$$\phi_1^\beta = \sum_{i=1}^{m}\phi_i^\beta = \sum_{i=1}^{m}\frac{\phi_i^0\exp(\sigma_1 Z_i)}{1 + V_\beta[\exp(\sigma_1 Z_i) - 1]} \quad (8)$$

Similarly, the composition of polymer 2 in α and β phases is

$$\phi_2^\alpha = \sum_{j=1}^{n}\phi_j^\alpha = \sum_{j=1}^{n}\frac{\phi_j^0}{1 + V_\beta[\exp(\sigma_2 Z_j) - 1]} \quad (9)$$

$$\phi_2^\beta = \sum_{j=1}^{n}\phi_j^\beta = \sum_{j=1}^{n}\frac{\phi_j^0\exp(\sigma_2 Z_j)}{1 + V_\beta[\exp(\sigma_2 Z_j) - 1]} \quad (10)$$

ANALYSIS OF THE EVOLUTION OF THE PHASE-SEPARATION PROCESS

The evolution of the phase-separation process at a constant temperature of 177 °C is determined by the solution of eqs 3, 4, and 6 as follows. For a certain value of p, with distribution functions for polymer 1 and 2 used previously and with the values of b and $D(T)$ determined in part 1 of this work[6] ($b = 0.7120 - 0.0809p - 1.3610p^2$ and $D_{177°C} = 0.13985 - 0.23821p$), the system of equations is numerically solved, and V_β, σ_1, and σ_2 are obtained. Knowing the species distribution in each phase, we calculated the values of r, p, the weight-average molecular weight, the density (ρ), and the composition separately for each phase. r in a particular phase is defined as follows:

$$r = \frac{\text{Total amino hydrogen equivalents}}{\text{Total epoxy equivalents}} \quad (11)$$

where *total* means the sum of reacted and unreacted equivalents.

At the beginning of the polymerization, the system with 60 wt % PS (i.e., $\Phi_2 = 0.634$) is homogeneous. As the reaction proceeds, the system becomes less miscible, and at a certain conversion level (cloud-point conversion = 0.265), the system becomes phase-separated. At this point, the composition of the continuous phase (i.e., the α phase) is the initial one due to the NG mechanism, and V_β is equal to zero because of the incipient conditions of the phase-separation process. The separation factors are $\sigma_1 = 0.1003$ and $\sigma_2 = -0.0228$. The calculated parameters for each phase are shown in Table 1. T1

The segregated phase, that is, the β phase, has a large amount of epoxy–amine polymer, and the

Author Proof

Table 1. Cloud-Point Parameters[a]

	α Phase	β Phase
ϕ_2	0.634	4.67×10^{-4}
p	0.265	0.4646
M_{w_1}	831.16	2041.76
M_{w_2}	3.24×10^5	8922.17
r	1	1.1389
ρ	1.099	1.206

[a] M_{w_1} = weight-average molecular weight of component 1 (epoxy–amine); M_{w_2} = weight-average molecular weight of component 2 (PS).

conversion in this phase is higher than that of the continuous phase. This is a result of the polymer fractionation, and high-molecular-weight species of the epoxy polymer are segregated into the dispersed phase. This fractionation arises from the difference in size (entropic effect) because it was previously assumed that the interactions between the epoxy–amine species and PS segments could be described by a single interaction parameter independently of the amount of epoxy (K) and amine (H) molecules incorporated into a particular $E_{H,K}$ species. Because of the higher functionality of the diamine monomer with respect to the diepoxide monomer, the first has a greater probability of reacting, and the segregated phase shows an increase in the amine/epoxy ratio. Figure 1 shows the mass fraction distribution of less reactive $E_{H,K}$ species. Because σ_2 is negative, only low-molecular-weight oligomers of PS are segregated into the dispersed phase. Figure 2 shows corresponding mass fraction distributions. F1 F2

After the cloud point, two kinds of strategies were used. The simplest one represents a case in which no diffusional limitations are present; that is, mass transfer proceeds at a much faster rate than polymerization, driving the system toward

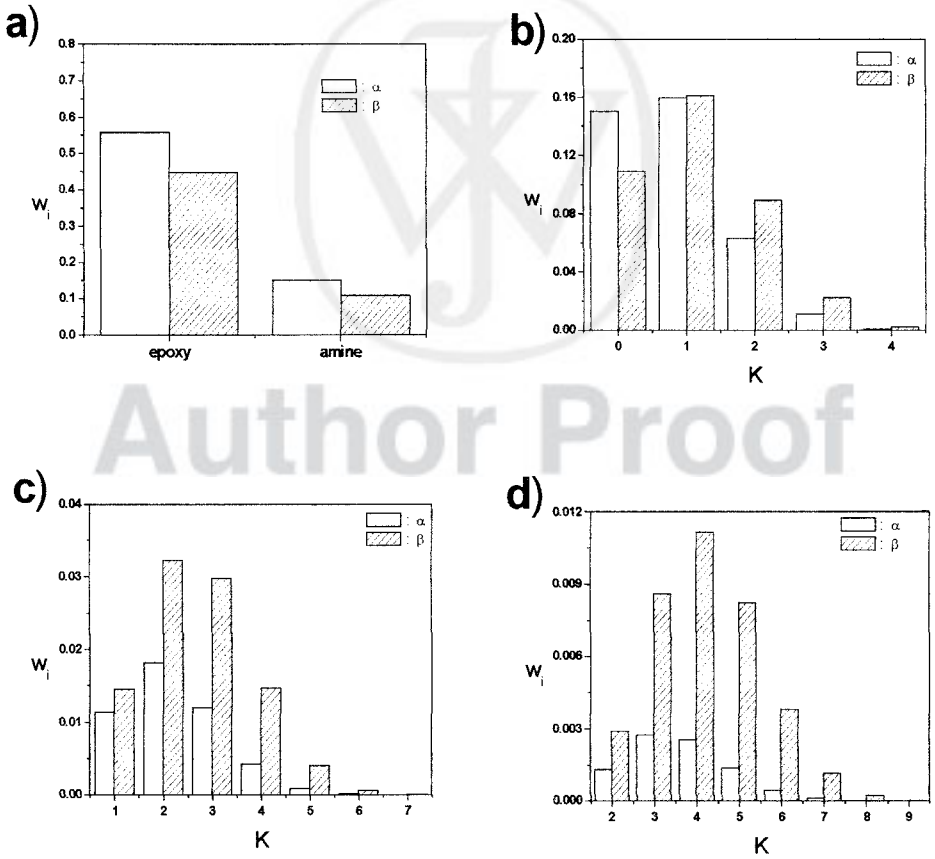

Figure 1. Mass fraction distributions of less reactive $E_{H,K}$ species at the cloud point: (a) diepoxide ($E_{1,0}$) and diamine ($E_{0,1}$) monomers, (b) $E_{1,K}$ species, (c) $E_{2,K}$ species, and (d) $E_{3,K}$ species.

Author Proof

tapraid5/z8q-polyphy/z8q-polyphy/z8q00604/z8q2785d04g | gockleyj | S=15 | 12/17/03 | 13:51 | Art: 03090532 | Input-DCT-???

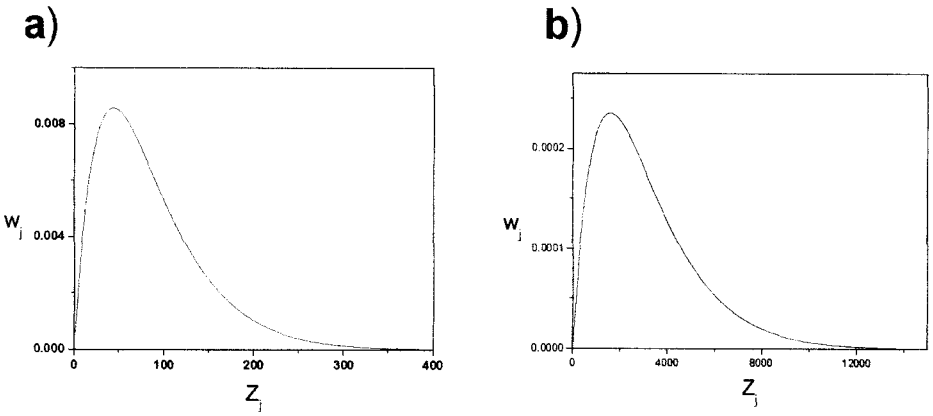

Figure 2. Mass fraction distributions of PS oligomers at the cloud point: (a) epoxy-rich phase (β phase) and (b) PS-rich phase (α phase).

equilibrium for any conversion. This strategy is wrong because it predicts $V_\beta = 0.0278$ for $p = 0.5$, whereas the experimental surface fraction of the dispersed epoxy-rich domains measured by Meynie et al.[5] was 0.223 for $p = 0.441$.

The second strategy considers that the β phase is semipermeable. As the epoxy-rich phase has a higher conversion than that of the PS-rich phase, epoxy–amine molecules will remain trapped in the dispersed domains. Therefore, the β phase will receive material from the continuous phase but will not deliver molecules back to the α phase. For this case, the thermodynamic simulation was carried out as follows. Once the α and β phases were generated, both phases reacted independently during a differential time, and the α phase was driven to equilibrium, segregating a differential amount of material that was incorporated into the β phase. At this stage, the β phase was modified both by the material received from the α phase and by the evolution of species via continuation of the polymerization. As the phase-separation process produced a stoichiometric imbalance because of the polymer fractionation, the molar concentration of generic $E_{H,K}$ species could not be calculated from the Stockmayer ideal distribution function. The distribution of chemical species during polymerization was generated from the corresponding kinetic equations, as reported in a previous article.[14]

In Figure 3, the predicted values of V_β versus the overall conversion ($\bar{p}$) are shown, along with the experimental surface fraction of the dispersed-phase particles. The good agreement indicates the accuracy of the strategy. The dashed part of the curve shows that these values are extrapolated because of the impossibility of calculating the conversion in the β phase with accuracy. Note that the experimental data were collected during the isothermal-polymerization-induced phase separation of a 60/40 PS/DGEBA–MDEA system at 177 °C under static and dynamic conditions.[5] The experimental $\bar{p}$ value at the cloud point was 0.27, and it was between 0.56 and 0.63 at the gel point.[5]

In Figure 4, the evolution of p is plotted versus $\bar{p}$. Initially, the α-phase conversion decreases as a result of the polymer fractionation: high-molecular-weight species are segregated into the β phase. Then, it increases because of the decreased differential volume fraction segregated in each step.

The composition of each phase, expressed as Φ_2, is shown in Figure 5. For $\bar{p}$ values greater

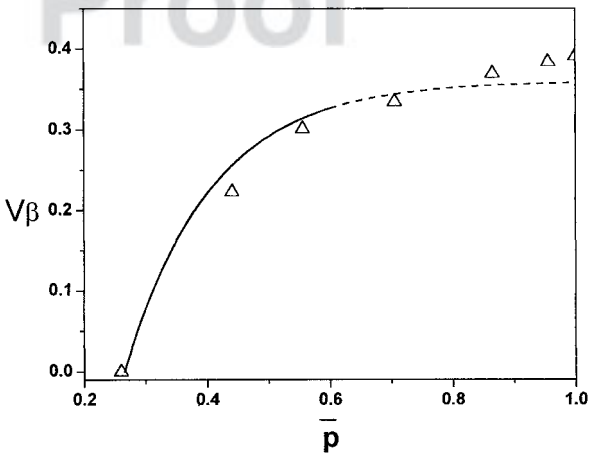

Figure 3. (—) Predicted V_β values and (△) experimental surface fractions of the dispersed phase.

Author Proof

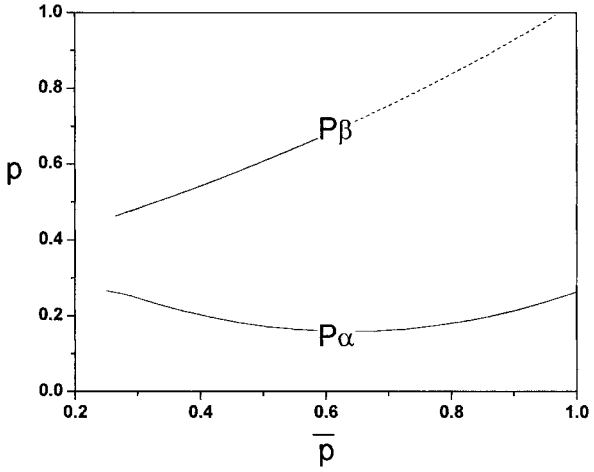

Figure 4. Evolution of p in each phase versus $\bar{p}$.

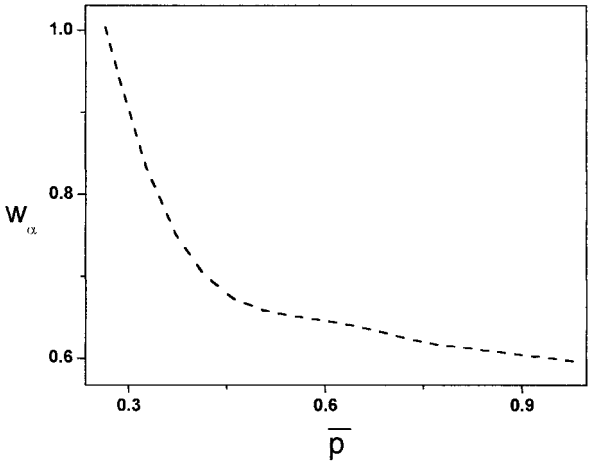

Figure 6. Mass fraction of the epoxy-rich phase (w_α) versus $\bar{p}$.

than 0.8, the continuous phase has less than 1% epoxy–amine polymer, and finally the segregation is almost complete. The same effect, as shown in Figure 6, can be noted in the representation of the mass fraction of the continuous phase: it is close to 0.6 at complete conversion.

The stoichiometric ratio in the β phase (r_β) of the epoxy–amine polymer is plotted in Figure 7. The β phase is initially enriched in the amino-hydrogen, but at a higher conversion, the epoxy groups prevail over the amine hydrogens. This is due to the high functionality of the amine monomer.

The molecular weight of PS in the β phase decreases with $\bar{p}$ because of PS fractionation, as shown in Figure 8.

MODELING THE EVOLUTION OF T_g AFTER PHASE SEPARATION IN THE α AND β PHASES

Knowing the concentration and composition of each phase, we can predict T_g of both phases by using the Couchman equation[15] and by considering that each phase is homogeneous. That is,

$$\ln T_g(\alpha) = \frac{w_{1(\alpha)}\Delta C_{p1(\alpha)} \ln T_{g1(\alpha)} + w_{2(\alpha)}\Delta C_{p2} \ln T_{g2}}{w_{1(\alpha)}\Delta C_{p1(\alpha)} + w_{2(\alpha)}\Delta C_{p2}} \tag{12}$$

$$\ln T_g(\beta) = \frac{w_{1(\beta)}\Delta C_{p1(\beta)} \ln T_{g1(\beta)} + w_{2(\beta)}\Delta C_{p2} \ln T_{g2}}{w_{1(\beta)}\Delta C_{p1(\beta)} + w_{2(\beta)}\Delta C_{p2}} \tag{13}$$

Author Proof

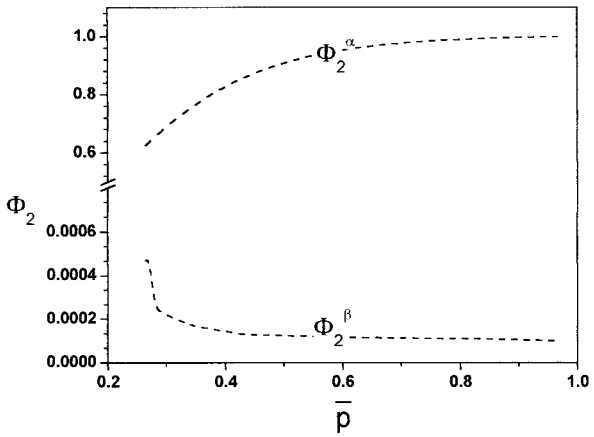

Figure 5. Φ_2 for each phase versus $\bar{p}$.

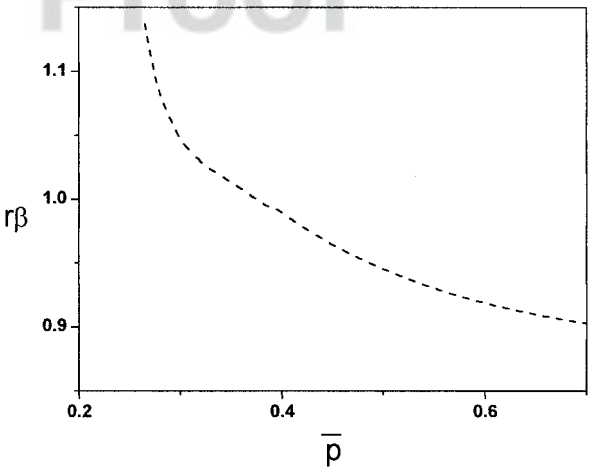

Figure 7. Evolution of r_β.

tapraid5/z8q-polyphy/z8q-polyphy/z8q00604/z8q2785d04g | gockleyj | S=15 | 12/17/03 | 13:51 | Art: 03090532 | Input-DCT-???

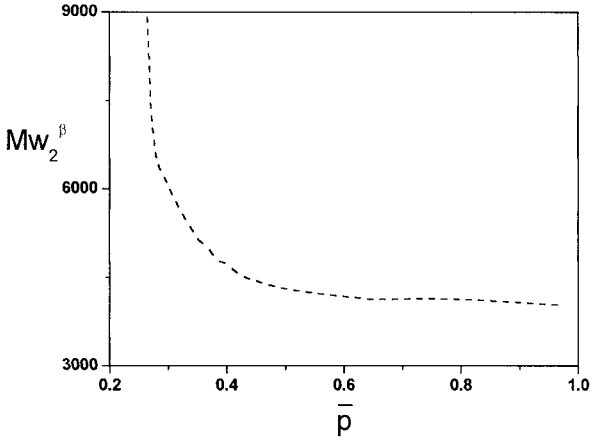

Figure 8. Weight-average molecular weight of P S in the epoxy-rich phase ($M^{\beta}_{w_2}$).

where w is the mass fraction of each component in each phase. T_g and the heat capacity change at T_g (ΔC_p) of component 1 (epoxy–amine) change with the conversion in each phase, whereas they are constant for component 2 (PS). The p values of α and β phases were predicted with the thermodynamic model. The experimental values of T_g for the neat and stoichiometric epoxy–amine systems are shown in Figure 9, and they can be modeled with the DiBenedetto equation:[16]

F9

$$\frac{T_g - 247}{438.5 - 247} = \frac{0.227p}{1 - (1 - 0.227)p} \qquad (14)$$

In Figure 10, the empirical correlation of the experimental ΔC_p values of the neat stoichiometric epoxy–amine system is plotted as a function of p.

F10

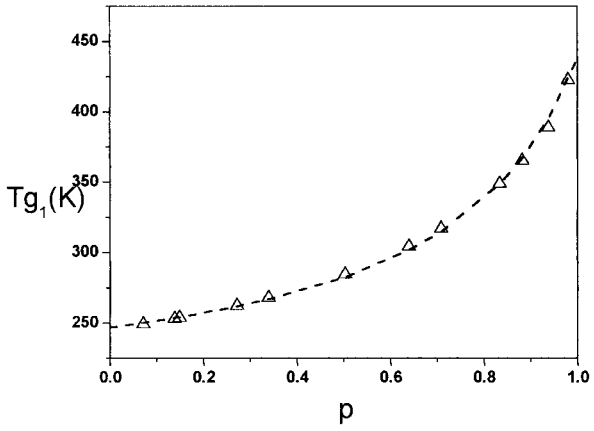

Figure 9. T_g of the neat epoxy–amine system.

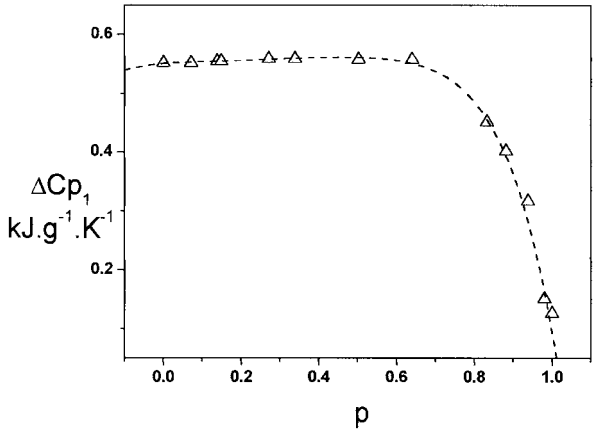

Figure 10. ΔC_p of the neat epoxy–amine system.

With eqs 12 and 13, T_g values of both phases have been predicted and plotted in Figure 11, along with experimental results. The agreement is good, but the experimental points are a little to the right of the T_g curves. This may be because the effect of r on T_g was not taken into account and because of the difficulty of obtaining the β distribution at a high total conversion.

F11

To predict ΔC_p values of both phases, we can use the following equations:

$$\Delta C_p(\alpha) = w_{1(\alpha)}\Delta C_{p1_{(\alpha)}} + w_{2(\alpha)}\Delta C_{p_2} \qquad (15)$$

$$\Delta C_p(\beta) = w_{1(\beta)}\Delta C_{p1_{(\beta)}} + w_{2(\beta)}\Delta C_{p_2} \qquad (16)$$

These equations agree with those published by Couchman[17] for the particular case in which the term that takes into account the interaction be-

Author Proof

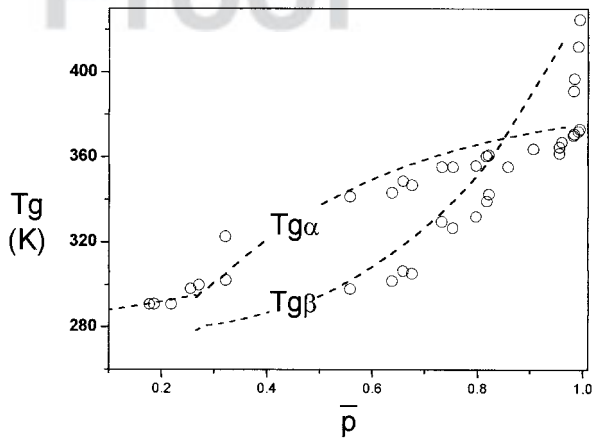

Figure 11. Experimental and predicted T_g values of both phases.

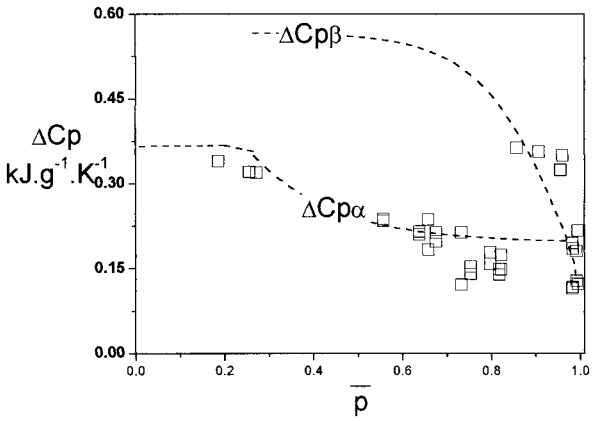

Figure 12. Experimental and predicted ΔC_p values of both phases.

tween the two polymers is negligible. The agreement between the predictions and experimental values is good despite the dispersion of the experimental results (Fig. 12). F12

CONCLUSIONS

A thermodynamic simulation of the phase-separation process of an off-critical blend, based on a thermoplastic matrix with a reactive system undergoing polymerization at a constant temperature, has been performed. The model considers the composition dependence of $\chi(T,\Phi_2)$ and the polydispersity of both polymers. For every level of conversion, the simulation has provided the amount, composition, r value, and conversion of each phase present.

At the beginning of the polymerization, the system is homogeneous. As the reaction proceeds, the system becomes less miscible, and at a certain conversion level, the cloud-point conversion, the system becomes phase-separated. At this point, the composition of the continuous α phase is the initial one, and the volume fraction of the β-dispersed phase is zero. The segregated phase has a large amount of the epoxy–amine polymer, and the conversion in this phase is higher than that of the continuous phase as a result of the polymer fractionation due to the entropic effect. Because of the higher functionality of the diamine monomer with respect to the diepoxide monomer, the first has a greater probability of reacting, and the segregated phase shows an increase in the amine/epoxy ratio. Only low-molecular-weight oligomers of PS are segregated into the dispersed phase.

After the cloud point, it is thought that the epoxy-rich phase is semipermeable. This signifies that the β phase will receive material from the continuous phase but will not deliver molecules back to the α phase. As the phase-separation process produces the polymer fractionation, the β phase is initially enriched in the amino-hydrogen, but at a higher conversion, the epoxy groups prevail over the amine hydrogens, and the molecular weight of PS in this phase decreases. Initially, the α-phase conversion decreases as a result of the polymer fractionation: high-molecular-weight epoxy species are segregated into the β phase. Then, it increases because of the reduction of the differential volume fraction segregated in each step. Finally, the segregation is almost complete, and the mass fraction of the continuous phase is close to that of the initial composition.

The accuracy of the model is proved by the good agreement between the experimental and predicted T_g and ΔC_p values for both phases.

REFERENCES AND NOTES

1. Venderbosch, R. W.; Meijer, H. E. H.; Lemstra, P. J. Polymer 1995, 36, 2903.
2. Sperling, L. E. Polymeric Multicomponent Materials: An Introduction; Wiley: New York, 1997.
3. Bonnet, A.; Pascault, J. P.; Sautereau, H.; Taha, M.; Camberlin, Y. Macromolecules 1999, 32, 8517.
4. Tran-Cong, Q. Structure and Properties of Multiphase Polymeric Materials; Marcel Dekker: New York, 1998; Chapter 5.
5. Meynie, L.; Fenouillot, F.; Pascault, J. P. Polymer, in press. AQ: 1
6. Riccardi, C. C.; Borrajo, J.; Meynie, L.; Fenouillot, F.; Pascault, J. P. J Polym Sci Part B: Polym Phys 2004, 42. AQ: 2
7. Riccardi, C. C.; Borrajo, J.; Williams, R. J. J. Polymer 1994, 35, 5541.
8. Holliday, L. In Composites Materials; Holliday, L., Ed.; Amsterdam, 1966; pp 1–27. AQ: 3
9. Qian, C.; Mumby, S. J.; Eichinger, B. E. Macromolecules 1991, 24, 1655.
10. Bae, Y. C.; Shim, J. J.; Soane, D. S.; Prausnitz, J. M. J Appl Polym Sci 1993, 47, 1193.
11. Bae, Y. C.; Lambert, D. S.; Soane, D. S.; Prausnitz, J. M. Macromolecules 1991, 24, 4403.
12. Choi, J. J.; Bae, Y. C. Fluid Phase Equilib 1999, 157, 213.
13. Koningsveld, R.; Kleintjens, L. A. J Polym Sci 1977, 61, 221. AQ: 4
14. Riccardi, C. C.; Borrajo, J. Polym Int 1993, 32, 241.
15. Couchman, P. R. Macromolecules 1978, 11, 1156.
16. Pascault, J. P.; Williams, R. J. J. J Polym Sci Part B: Polym Phys 1990, 28, 85.
17. Couchman, P. R. Macromolecules 1991, 24, 5772.

Author Proof